Proceedings of *The Riddle of Cooling Flows in Galaxies and Clusters of Galaxies*
May 31 – June 4, 2003, Charlottesville, Virginia, USA
Ed. T. H. Reiprich, J. C. Kempner, & N. Soker

Chandra Observation of the Core of Abell 576

Joshua C. Kempner[1] and Laurence P. David[1]

[1] *Harvard-Smithsonian Center for Astrophysics, 60 Garden St., MS-67, Cambridge, MA 02138*

We present data from a *Chandra* observation of the nearby cluster of galaxies Abell 576. The core of the cluster shows a significant departure from dynamical equilibrium. We show that this core gas is most likely the remnant of a merging subcluster, which has been stripped of much of its gas, depositing a stream of gas behind it in the main cluster. The unstripped remnant of the subcluster is characterized by a different temperature, density and metalicity than that of the surrounding main cluster, suggesting its distinct origin. Continual dissipation of the kinetic energy of this minor merger may be sufficient to counteract most cooling in the main cluster over the lifetime of the merger event.

1. Introduction

With its low redshift, Abell 576 makes excellent use of the capabilities of *Chandra*, allowing us to examine in detail the very core of the cluster. We focus here on the dynamical activity in the core of cluster. The cluster shows strong evidence, first suggested by Mohr et al. (1996) from an analysis of the galaxy population, of the remnant core of a small merged subcluster. We demonstrate that the X-ray data are consistent with this picture, and even suggest it as the most likely origin for the non-equilibrium gas at the center of Abell 576. In fact, the subcluster may still be in the process of settling into the center of the main cluster's potential.

We present 27.9 kiloseconds of *Chandra* ACIS-S data (OBSID 3289). The data have been corrected for CTI and the particle background reduced using the standard procedure for data taken in Very Faint mode. Background corrections were performed using blank sky files provided in the CALDB. For the spectroscopic analysis we considered only data in the range 0.5–8 keV. The arfs were corrected for the reduction in quantum efficiency at low energies using the *acisabs* model.

We assume $H_0 = 71$, $\Omega_m = 0.27$, and $\Omega_\Lambda = 0.73$, so $1'' = 0.738$ kpc at the redshift of A576 ($z = 0.0377$). All errors are quoted at 90% confidence unless otherwise stated.

2. Brightness Edges

Figure 1 shows a Gaussian smoothed, exposure-corrected image of the cluster. At least two, and perhaps more, surface brightness edges are visible within the central 50 kpc. As shown below, they encompass a region of cool, high-metalicity gas. This cool gas also extends in a finger to the north of the cluster core, slightly west of center. As we will discuss in the remainder of this section, we believe this finger of gas to have originated in a small subcluster which is currently accreting into the center of the main cluster. The orientation of the edges are not consistent with gas simply sloshing back and forth in a more or less fixed potential, which would create parallel edges, but are more consistent with being the outer edges of a wake of stripped gas left behind by a merging subcluster. This hypothesis also neatly explains the finger of gas to the north, which cannot be easily explained by simple sloshing.

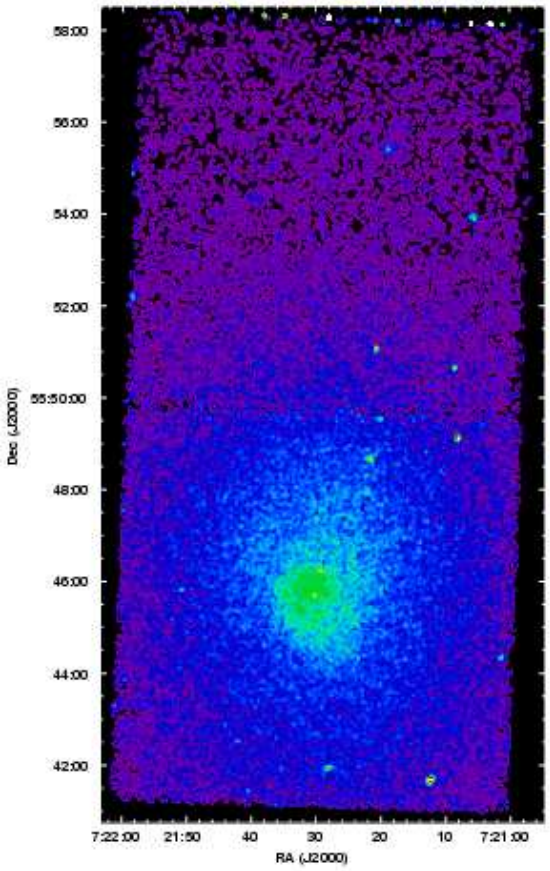

FIG. 1.— Gaussian smoothed, exposure-corrected, 0.3–6.0 keV image of Abell 576. Both the S2 and S3 chips are shown. The north and southeast surface brightness edges are clearly visible; the west edge is less distinct.

We extracted surface brightness and spectral profiles across all three edges. The brightness edge $40''$ north of the peak of the X-ray emission shows by far the largest jump in surface brightness: a factor of 1.8 ± 0.15 (1σ)

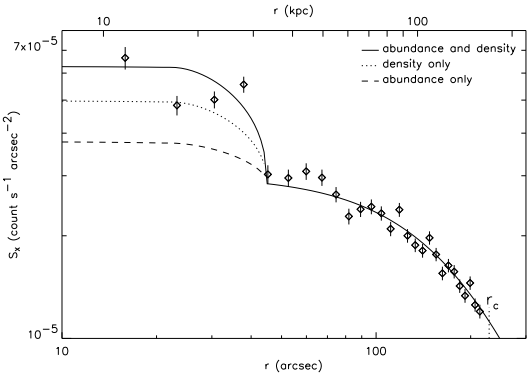

FIG. 2.— Surface brightness profile across the north edge. The solid line outside 30 kpc is a beta model fit to the data using the parameters derived by Mohr et al. (1995) using the full field of view of the *Einstein* IPC. Inside 30 kpc, three models for the surface brightness jump are shown: the solid line indicates the same beta model after adjusting for the enhancement due to both the density and abundance increases inside the edge. The abundance only and density only components are shown as the dashed and dotted lines, respectively . For the β-model, $\beta = 0.64$ and $r_c = 169$ kpc. The core radius of the model is indicated as "r_c" for reference. The errors bars are 1σ.

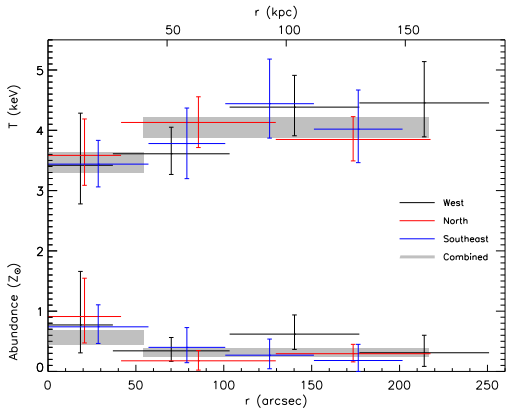

FIG. 3.— Spectral profiles in three sectors to the north, southeast, and west from the cluster center. The top set of points are temperatures; the bottom set are abundances. All error bars are 90% confidence.

increase across the discontinuity (see Figure 2). A large jump in the abundance is also visible across the discontinuity, while the temperature does not change significantly (see the red points in Figure 3). At the low temperature of Abell 576, the increased abundance across the edge has a non-negligible effect on the emissivity of the gas. This is illustrated in Figure 2, which shows the surface brightness profile across the north edge. Outside the brightness edge, the solid line is a β-model fit to the data using the core radius and slope determined from observations with *Einstein* (Mohr et al. 1996). Inside the edge, we use the same β-model, but we increase the emissivity by an amount expected from each of three different models: the dotted line indicates the increased surface brightness due to the increase in density; the dashed line indicates the increase due to the higher abundance, and the solid line is the increased brightness due to both effects. For all three models we assume spherical symmetry for consistency with the deprojection analysis. As the figure demonstrates, neither the added emissivity from the higher abundance nor that from the increased density can account entirely for the observed increase in surface brightness, but the two effects combined reproduce the overall normalization of the central brightness quite well.

We deprojected the surface brightness, which, when combined with the temperature and abundance profiles, allowed us to determine deprojected density and pressure profiles across the edge, under the assumption of spherical symmetry. We find a small jump in both the density and the pressure across the north edge. The density increases by a factor of $2.8^{+0.8}_{-1.2}$ while the pressure increases by a factor of 2.4 ± 0.5 (both 1σ). In order for the higher density gas to remain confined, the pressure difference across the edge must be balanced by ram pressure from motion of the high density gas through the lower density gas. The observed pressure difference implies that the higher density gas is moving through the lower density gas with a velocity of 750 ± 270 km s^{-1}, or Mach 0.9 ± 0.3 at the sound speed of the lower density gas (both errors are 1σ). The velocity we measure is consistent with velocities of both merging/accreting subclusters measured in other clusters (e.g. Markevitch et al. 2000) and with velocities measured for some "sloshing" edges in the cores of relaxed clusters (Markevtich 2003). On its own, then, the measured velocity of the north edge is incapable of distinguishing between these two scenarios for the creation of the non-hydrostatic features in the cluster core.

To the southeast of the cluster center, a fainter edge is visible in the image (see Figure 1). Another yet fainter edge appears to the west. Both of these edges display the same abundance gradient as the north edge, though in both cases the abundance jump appears to be more of a gradient than a sharp edge, and is measured with much less significance (see Figure 3).

3. Suppression of Cooling

As Figure 3 shows, the temperature drops in the very core of the cluster, that is, inside the brightness edge. It is natural to ask, then, if this gas shows any evidence of being multi-phase. To test this, we fit a spectrum of the gas in the core with a single-temperature absorbed MEKAL model (Kaastra 1992), with a MEKAL model plus a multi-phase MEKAL model (MKCFLOW model), and with the sum of two MEKAL models. Application of the F-statistic shows the cooling flow model to be a marginally better fit than the single-phase model, and the two-temperature model to be an even better fit, although none is so much better as to be considered preferred over the others.

The spectroscopic cooling rate we measure is quite low: an order of magnitude smaller than the "classical cooling flow" accretion rate of $\dot{M} = M/t_{\rm cool} = 11$ M$_\odot$ yr^{-1} derived from the gas mass and cooling time in the inner 30 kpc (see Figure 4). We should note that the cool component in the two-temperature model only contributes $\sim$0.1% to the overall normalization of the model. This is consistent with the extremely small cooling rate mea-

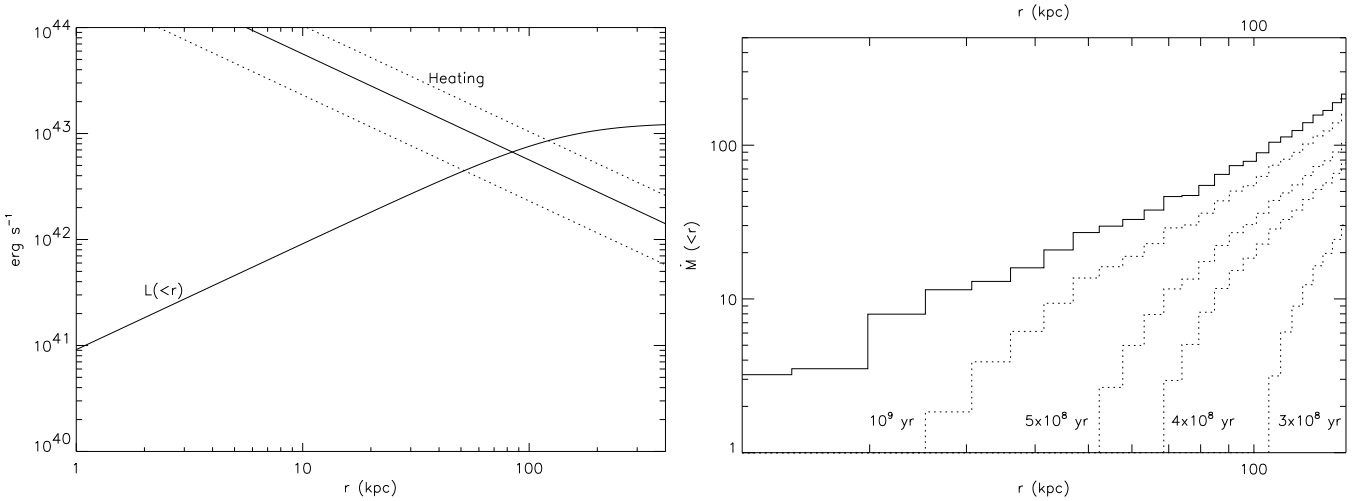

FIG. 4.— *(a)* Heating rate and luminosity of radiative cooling as a function of radius. The exact definition of the heating rate is given in the text. The dotted curves indicate the minimum and maximum allowed rates given the errors on our measurement of the subcluster's velocity. *(b)* Integrated cooling rate as a function of radius. The solid line is the rate in the absence of heating. The dotted lines are the resulting integrated cooling rate if the kinetic energy of the cool core is dissipated over the given timescales. The dissipated energy is assumed to heat the gas at a constant rate per volume over the entire region.

sured for the cooling flow model. In short, we find very marginal evidence of multi-phase gas in the central cool core.

Given that we observe essentially no cooling in either the core or outside the core in what is otherwise a quite relaxed cluster, we now explore whether the dissipation of the kinetic energy of the remnant core is capable of suppressing cooling at the observed level. We assume for this discussion that the merging subcluster explanation of the brightness edges is correct.

We determined the kinetic energy of the gas inside the north edge using the velocity of the edge we measured above plus a gas mass determined from the deprojected density profile inside the edge ($\sim 2\times10^{10}$ $M_\odot$). We then calculated the rate of energy input from the dissipation of this kinetic energy over a variety of timescales. Figure 4a shows this energy dissipation rate compared to the luminosity due to radiative cooling as a function of radius. The timescale used for calculating the heating rate is three crossing times of the cluster to the given radius at the current velocity of the north edge. In three crossing times, the moving cool core will have swept up its mass in gas, reducing its kinetic energy by 3/4. We therefore assume perfectly efficient thermalization of 3/4 of the kinetic energy over a timescale equal to three crossing times by the core at its current velocity in calculating the heating rate.

If we take the point at which the west and southeast edges converge as indicative of the current orbital radius of the subcluster (∼100 kpc from the cluster center), the dissipation timescale derived using the above method is 4×10^8 years. As can be seen from Figure 4b, the heating simply from the dissipation of the kinetic energy of the subcluster is capable of suppressing cooling by a factor of more than 4 in the inner 100 kpc over this timescale. If the dissipation of the core's kinetic energy is spread out over 10^9 years, cooling can still be suppressed at the level observed in the inner 30 kpc.

Support for this work was provided by the National Aeronautics and Space Administration through *Chandra* Award Number G01-2131X issued by the *Chandra* X-ray Observatory Center, which is operated by the Smithsonian Astrophysical Observatory for and on behalf of NASA under contract NAS8-39073, and by NASA contract NAG5-12933.

References

Kaastra, J. S. 1992, An X-Ray Spectral Code for Optically Thin Plasmas, Tech. rep., Internal SRON-Leiden Report, updated version 2.0

Markevitch, M., Ponman, T. J., Nulsen, P. E. J., Bautz, M. W., Burke, D. J., David, L. P., Davis, D., Donnelly, R. H., Forman, W. R., Jones, C., Kaastra, J., Kellogg, E., Kim, D.-W., Kolodziejczak, J., Mazzotta, P., Pagliaro, A., Patel, S., Van Speybroeck, L., Vikhlinin, A., Vrtilek, J., Wise, M., & Zhao, P. 2000, ApJ, 541, 542

Markevtich, M. 2003, these proceedings

Mohr, J. J., Evrard, A. E., Fabricant, D. G., & Geller, M. J. 1995, ApJ, 447, 8

Mohr, J. J., Geller, M. J., Fabricant, D. G., Wegner, G., Thorstensen, J., & Richstone, D. O. 1996, ApJ, 470, 724